Hindawi Publishing Corporation
Advances in Condensed Matter Physics
Volume 2015, Article ID 206501, 7 pages
http://dx.doi.org/10.1155/2015/206501

Research Article

(112) Surface of $CuInSe_2$ Thin Films with Doped Cd Atoms

Bo Yin and Chaogang Lou

School of Electronic Science and Engineering, Southeast University, Nanjing 210096, China

Correspondence should be addressed to Chaogang Lou; lcg@seu.edu.cn

Received 2 September 2014; Revised 26 December 2014; Accepted 6 January 2015

Academic Editor: Dario Alfe

The doping behavior of Cd atoms in the $CuInSe_2$ thin films and their influences on electronic structures are investigated. The doped Cd atoms replace Cu atoms and prefer to stay at the (112) surface of the thin films. They combine with Cu vacancies to form defect pairs due to low formation energy. The Cd atom does not by itself modify significantly the electronic structure of the surface, but the defect pairs have important influences. They result in a down shift of valence band maximum and form a hole barrier at the surface, which can prevent holes from reaching the surface and reduce the recombination of carriers.

1. Introduction

Chalcopyrite semiconductors such as $CuInSe_2$ (CIS) and $CuInGaSe_2$ (CIGS) are important photovoltaic materials. They are used as the absorber of the polycrystalline thin film solar cells which reached a high conversion efficiency record of 20.3% [1]. In this kind of solar cells, the surface of the chalcopyrite thin films plays a significant role because its atomic structure and the chemical composition have effects on the heterojunction of the solar cells and consequently influence their performance [2–6].

In past decades, the surface of the polycrystalline chalcopyrite thin film was investigated extensively [7–13]. Their stable surface is a polar (112) plane with defect-induced reconstruction [8]. Theoretical and experimental studies have found that the polar surface (112) is popular in the $CuInSe_2$ thin films due to their low surface energy [7, 9]. It has also been revealed that the surface layer of the films usually has Cu vacancies (V_{Cu}) which modify the electronic structure of the materials [3, 4, 14].

For the surface of the chalcopyrite thin films inside the CIS/CdS heterojunction, the situation becomes more complicated. According to previous works [15], the (112) surface inside the heterojunction will become more Cu deficient. Furthermore, the n-type CdS film which is on the (112) surface of the CIS films has chances to diffuse Cd atoms into the chalcopyrite thin films. So it is worthy to investigate how the doped Cd atoms influence the surface of the chalcopyrite thin films because it will improve our understanding about the mechanism of carrier transportation inside the chalcopyrite thin film solar cells.

In this paper, the model of surface of the CIS thin films with doped Cd atoms is built. By comparing the defect formation energies, the locations of Cd atoms are investigated. We have also calculated the influences of Cd doping on the electronic structures and the transportation of carriers.

2. Methodology

A defect-free (112) surface model is built, as shown in Figure 1. This is the basis of the next studies about the Cd doping. The crystal lattice parameters are set according to experimental values $a = 5.784$ Å, $c = 11.616$ Å, and $c/a = 2.0083$ [16]. These values are close to the first-determined experimental values ($a = 5.781$ Å, $c = 11.642$ Å, and $c/a = 2.0138$) [17]. Table 1 shows the calculated lattice parameters a, c, and c/a of CIS unit cell after the relaxation and the experimental values. The experimental values are also shown for comparison (the changes between the theoretical and experimental values are also shown in parentheses). The calculated lattice parameters of CIS ($a = 5.719$ Å, $c = 11.492$ Å, and $c/a = 2.0094$) have satisfactory agreement with the experimental values.

To investigate the locations of the Cd atoms, the complete model including seven atomic layers and 56 atoms is built, as shown in Figure 2. To prevent the charge-transfer

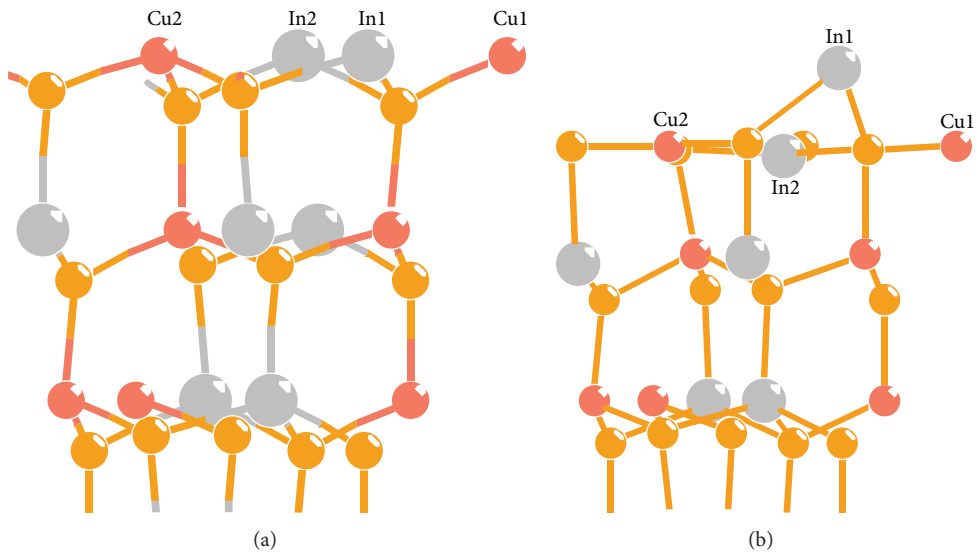

Figure 1: Atomic structure of the (112) surface: (a) the surface before atomic relaxation and (b) the surface after atomic relaxation. The red, gray, and yellow balls represent Cu, In, and Se atoms, respectively.

Table 1: The theoretical lattice parameters a, c, and c/a of CIS unit cell and the experimental values.

	Space group	a (Å)	c (Å)	c/a
Experimental (before relaxation) [16]	$I\bar{4}2d$	5.784	11.616	2.0083
Experimental [17]		5.781	11.642	2.0138
Theoretical (after relaxation)		5.719 (−1.1%)	11.492 (−1.1%)	2.0094

Table 2: The values of band angles in the relaxed (112) surface.

Bond type	Bond angle (°)			Average (°)
Se-Cu 1-Se	114.79	129.43	115.78	120.00
Se-Cu 2-Se	127.95	124.59	107.43	119.99
Se-In 1-Se	82.56	83.53	88.58	84.89
Se-In 2-Se	122.75	119.85	116.74	119.78

between the top layer and bottom layer of the slab, we use pseudohydrogen to passivate the bottom layer. The surface structure was optimized by atomic relaxation. The formation energies are calculated to determine the possible locations of the doping Cd atoms in the slab. We also investigated the influences of Cd doping on the electronic structure by calculating the density of state (DOS).

All calculations, including geometry optimization and total energy calculation, are based on the density-functional theory [18, 19]. We used the functional CA-PZ [20, 21] (the Perdew and Zunger parameterization of the numerical results of Ceperley and Alder) of local density approximation (LDA) [22] and the ultrasoft pseudopotential [23] plane-wave method [24]. The cutoff energy for the plane-wave basis is set as 310 eV, and for the first Brillion zone, $3 \times 4 \times 1$ k-point grids are used for all structures. During the geometry optimization, the two bottom atomic layers of the slab were fixed, and the atoms in the top five layers are relaxed until the forces are less than 0.03 eV/Å.

3. Results

3.1. The Atomic Relaxation of (112) Surface. For the defect-free (112) surface, after the relaxation, the atomic arrangement at the top surface layer is changed to reduce the total energy. Figure 1(b) shows the atomic structures after the relaxation. The two Cu atoms at the surface are denoted as "Cu1" and "Cu2," and the two In atoms are denoted as "In1" and "In2. The atoms Cu1 and Cu2 move down from the original positions, almost on the same plane with the Se atoms of the surface. However, the two In atoms have contradictory behaviors: the atom In1 moves up to become a top atom, and the atom In2 moves down, nearly in the plane of Cu1 and Cu2.

The reconstruction of the atomic structure can be explained by the crystal field theory and the valence-bond theory [25–27]. In CIS bulk materials, the Cu atom is the center of the tetrahedral structure which consists of the Cu atom and its four neighboring Se atoms. However, at the (112) surface, the Cu atom loses one neighboring Se atom, and the tetrahedral structure cannot be kept. In order to redistribute the electrons around Cu-Se bonds, the Cu atom and its three neighboring Se atoms form a new triangular structure and reach a stable state. This can be seen from the values of bond angle between Cu and Se atoms, as listed in Table 2.

In CIS the bonding between the atoms In and Se is mainly consisted of s and p orbital electrons of In and p orbital electrons of Se [27, 28]. The tetrahedral structure is formed by sp^3 hybridization, like the diamond cubic structure. After the relaxation, for the In atoms located at the surface, their positions are changed likely due to degenerated sp^3 hybridization

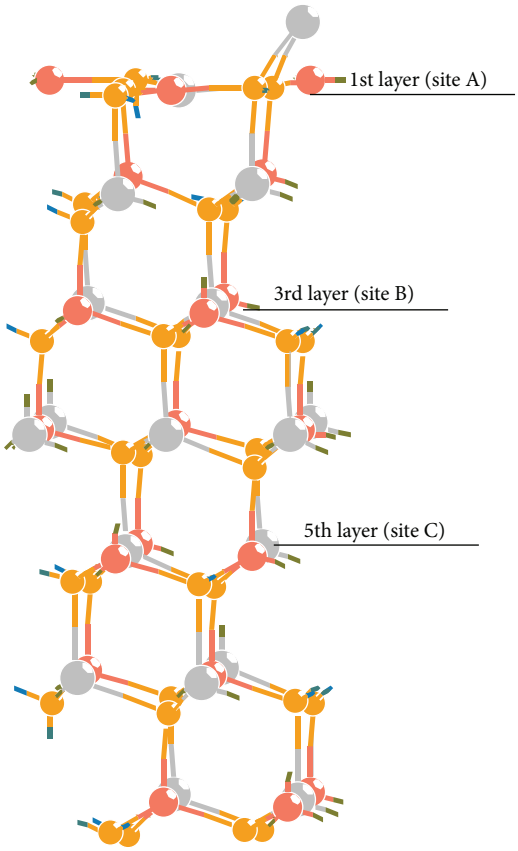

FIGURE 2: One defect Cd_{Cu} is located at three different sites along the direction [112], respectively, in the structure including 7 atomic layers and 56 atoms. The red, gray, and yellow balls represent Cu, In, and Se atoms, respectively.

according to the valence-bond theory [29, 30]. The degenerated hybridization of sp^3 has two directions: $sp^3 \rightarrow p^3 + s^1$ and $sp^3 \rightarrow sp^2 + p^1$. Correspondingly, the bond angles become 90° (p^3) and 120° (sp^2) from 109° (sp^3), respectively. From the data in Table 2, we can deduce that the rising In1 atom corresponds to $sp^3 \rightarrow p^3 + s^1$, and the lower In2 atom results from the degeneration $sp^3 \rightarrow sp^2 + p^1$.

To prove the relaxed results in Figure 1(b), we also built a 12-layer model. The optimization of geometry gives similar results.

3.2. Cd Doping at the (112) Surface. When the Cd atom enters into the CIS films, it may locate at the surface or migrate into a deeper position. Some experiments [31] reveal that the Cd atoms will replace the Cu and In atoms in the form of defects Cd_{Cu} and Cd_{In}. Because there exist many Cu vacancies in the CIS thin films, especially at the surface [4, 5], it is more possible that the Cd atom substitutes Cu instead of In. Here we consider only the defect Cd_{Cu}.

In order to clarify the position of the Cd atom in CIS thin film, we place the defect Cd_{Cu} at three different sites. (1) The defect Cd_{Cu} is arranged at the top surface layer (denoted as "1st layer" in Figure 2). (2) The defect Cd_{Cu} is located at the third layer. (3) The defect Cd_{Cu} is located at the fifth layer. For convenience, the three sites are named as "site A," "site B," and "site C," respectively. The formation energies of the defect at the three sites are calculated to clarify the distribution of Cd atom along the direction vertical to the surface (112).

In addition, considering that the Cu vacancies (denoted as V_{Cu}) are most likely located at the surface layer, it is possible that the defect Cd_{Cu} forms a defect pair with V_{Cu}, so we also calculate the formation energies of two kinds of defect pairs: (1) defects Cd_{Cu} and V_{Cu} are located closely to form defect pair $Cd_{Cu}^{+} + V_{Cu}^{-}$ at the surface layer; (2) the defect Cd_{Cu} is located at the surface layer, and the Cu vacancy is located at the second layer and not as close as the former. Both of them are shown in Figures 3(a) and 3(b). All the defective structures are based on the relaxed (112) surface structure discussed in Section 3.1.

To determine the favorite site of the defect Cd_{Cu}, we calculate the defect formation energies. For uncharged defect α, the formation energy is given by [15]

$$\Delta H(\alpha) = E_{\text{defect}} - E_{\text{ideal}} + n_i \mu_i. \tag{1}$$

Here E_{defect} is the total energy of the defective system and E_{ideal} is the total energy of the ideal system (defect-free surface). n_i is the number of the atoms which are added to/removed from the ideal structure. If the atoms are added, n_i is negative; if the atoms are removed, n_i is positive. μ_i is the chemical potential of an atom which is removed or added.

For the defect Cd_{Cu}, the expression of formation energy is rewritten as

$$\Delta H(Cd_{Cu}) = E_{\text{defect}} - E_{\text{ideal}} + \mu_{Cu} - \mu_{Cd}. \tag{2}$$

Here μ_{Cu} and μ_{Cd} are the chemical potentials of a Cu atom and a Cd atom, respectively.

For the defect pair $Cd_{Cu}^{+} + V_{Cu}^{-}$, the defect formation energy is

$$\Delta H(Cd_{Cu}^{+} + V_{Cu}^{-}) = E_{\text{defect}}^{\text{p}} - E_{\text{ideal}} + 2\mu_{Cu} - \mu_{Cd}. \tag{3}$$

Here $E_{\text{defect}}^{\text{p}}$ is the total energy of the defective system. To make the comparison easier, we defined a relative chemical potential $\Delta\mu_i$. For Cu and Cd atoms, the relative chemical potential can be written as

$$\begin{aligned} \Delta\mu_{Cu} &= \mu_{Cu} - \mu_{Cu}^{\text{solid}} \\ \Delta\mu_{Cd} &= \mu_{Cd} - \mu_{Cd}^{\text{solid}}. \end{aligned} \tag{4}$$

Here μ_{Cu}^{solid} is the chemical potential of Cu atom in the solid Cu (fcc) and μ_{Cd}^{solid} is the chemical potential of Cd atom in solid Cd (primitive hexagonal), which can be determined by calculations.

So (2) and (3) can be rewritten as

$$\begin{aligned} \Delta H(Cd_{Cu}) &= \left(E_{\text{defect}} - E_{\text{ideal}} + \mu_{Cu}^{\text{solid}} - \mu_{Cd}^{\text{solid}}\right) \\ &\quad + \Delta\mu_{Cu} - \Delta\mu_{Cd}, \\ \Delta H(Cd_{Cu}^{+} + V_{Cu}^{-}) &= \left(E_{\text{defect}}^{\text{p}} - E_{\text{ideal}} + 2\mu_{Cu}^{\text{solid}} - \mu_{Cd}^{\text{solid}}\right) \\ &\quad + 2\Delta\mu_{Cu} - \Delta\mu_{Cd}. \end{aligned} \tag{5}$$

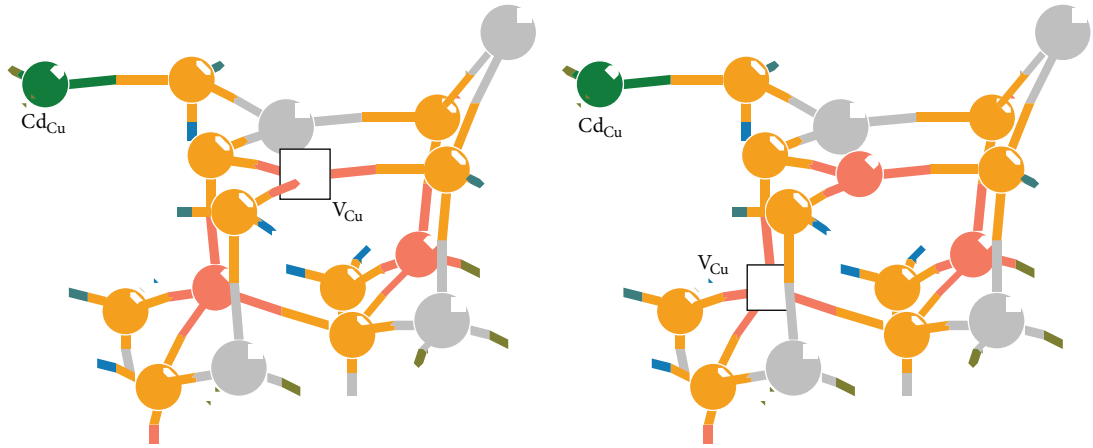

FIGURE 3: (a) The defect pair $Cd_{Cu}^{+} + V_{Cu}^{-}$ at the surface layer. (b) The two defects Cd_{Cu} and V_{Cu} at the different layers. The red, gray, and yellow balls represent Cu, In, and Se atoms, respectively. The squares represent Cu vacancies. The green ball is the Cd atom.

TABLE 3: Defect formation energy.

Defect position	ΔH (eV)
Site A	$0.651 + \Delta\mu_{Cu} - \Delta\mu_{Cd}$
Site B	$0.645 + \Delta\mu_{Cu} - \Delta\mu_{Cd}$
Site C	$0.544 + \Delta\mu_{Cu} - \Delta\mu_{Cd}$
$Cd_{Cu}^{+} + V_{Cu}^{-}$ at the surface	$-0.007 + 2\Delta\mu_{Cu} - \Delta\mu_{Cd}$
Cd_{Cu} and V_{Cu} at different layers	$0.428 + 2\Delta\mu_{Cu} - \Delta\mu_{Cd}$

According to (5), we can obtain the defect formation energies of Cd_{Cu} and the defect pair, as listed in Table 3.

In order to compare clearly the formation energies of the defects, it is needed to determine the values of $\Delta\mu_{Cu}$ and $\Delta\mu_{Cd}$. To simplify the calculation, we assume that the value of $\Delta\mu_{Cd}$ does not vary with the site of the Cd atom, so we just consider the variation of $\Delta\mu_{Cu}$.

In order to maintain a stable $CuInSe_2$ compound and avoid the precipitation of elemental solids (elements Cu, In, and Se), the relative chemical potential of Cu can vary in the intervals [15] as

$$\Delta H_f\left(CuInSe_2\right) \le \Delta\mu_{Cu} \le 0, \tag{6}$$

where $\Delta H_f(CuInSe_2)$ (−2.0 eV) is the formation energy of solid $CuInSe_2$ [15]. $\Delta\mu_{Cu} = 0$ corresponds to Cu-rich conditions and $\Delta\mu_{Cu} = -2.0$ corresponds to Cu-poor conditions. From the defect formation energies in Table 3 and (5)-(6), we can plot the curves of the formation energy versus the relative chemical potential $\Delta\mu_{Cu}$, as shown in Figure 4.

It can be seen that all formation energies of single defect and defect pair decrease when the relative chemical potential of Cu decreases, and this indicates that the defects are formed easier in Cu-poor environment than Cu-rich environment. The formation energy of the defect pair at the surface layer is the lowest.

For the single defect Cd_{Cu}, the formation energy at the deeper site (site C) is lower than that at the surface (site A).

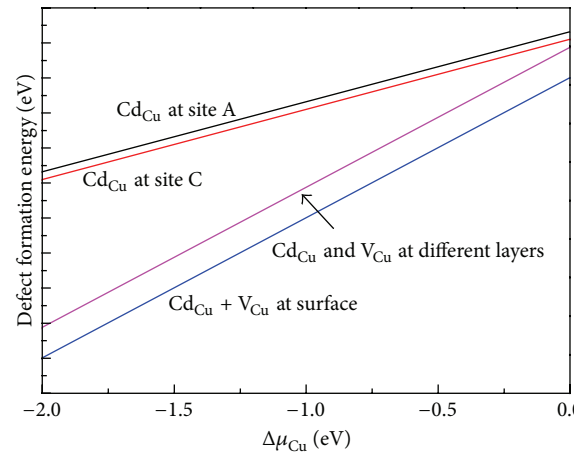

FIGURE 4: Defect formation energies versus the relative chemical potential $\Delta\mu_{Cu}$. $\Delta\mu_{Cu} = 0$ corresponds to Cu-rich conditions and $\Delta\mu_{Cu} = -2.0$ corresponds to Cu-poor conditions. Here we do not consider the variation of chemical potential of the Cd atom.

It means the Cd atoms may migrate into the deep layers of the CIS thin film. This agrees with the results [31–33] that Cd atoms diffuse approximately 100 Å~300 Å from the heterojunction boundary.

However, the defect pair $Cd_{Cu}^{+} + V_{Cu}^{-}$ at the surface layer has the lowest formation energy. The energy reduction can be attributed to the electrostatic interaction between Cd_{Cu} and V_{Cu} [15]. To clearly explain this, here we defined the interaction energy

$$\delta H_{int} = \Delta H\left(Cd_{Cu}^{+} + V_{Cu}^{-}\right) - \Delta H\left(V_{Cu}\right) - \Delta H\left(Cd_{Cu}\right). \tag{7}$$

Here δH_{int} is the energy change when two defects Cd_{Cu} and V_{Cu} are located closely to form a defect pair [15]. The term $\Delta H(V_{Cu})$ and $\Delta H(Cd_{Cu})$ are the formation energy of isolated

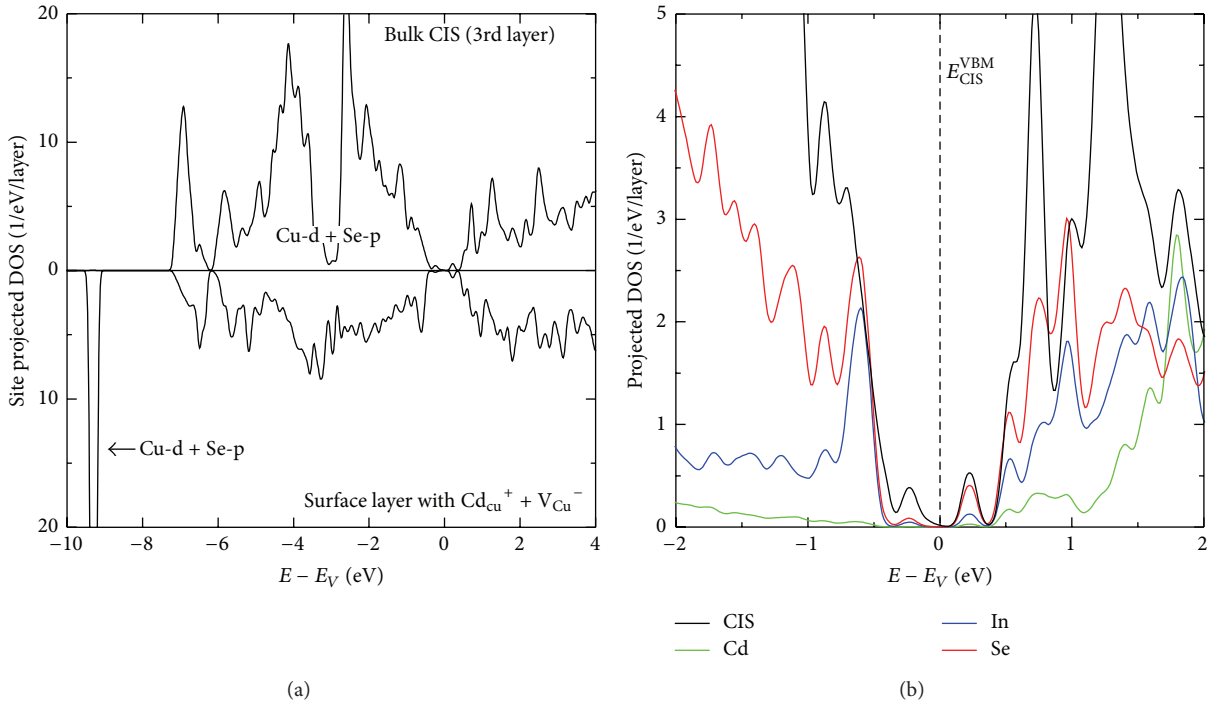

FIGURE 5: (a) The site projected density of states (PDOS) of the surface layer with defect pair $Cd_{Cu}^{+} + V_{Cu}^{-}$ (the lower panel) and the third layer (the upper panel). (b) PDOS of Cd, In, and Se atoms in the relaxed surface and the DOS of the third layer is shown for reference, marked as "CIS." The dash line in (b) represents the valence band maximum of the bulk CIS.

defect V_{Cu} and Cd_{Cu}, respectively. For the defect pair in the surface layer, the interaction energy δH_{int} can be calculated, and its value is −0.857 eV. When Cd_{Cu} and V_{Cu} are located at the different layers, the distance between them becomes longer, so their electrostatics interaction is weakened. The interaction energy becomes −0.422 eV when V_{Cu} and Cd_{Cu} are located at the surface and the second layer, respectively. Therefore, the Cd atoms prefer staying at the surface layer with the Cu vacancies to form the defect pair $Cd_{Cu}^{+} + V_{Cu}^{-}$.

3.3. Electronic Structure. The electronic structures were also investigated by the calculations of density of states (DOS). Figure 5(a) shows the site projected density of states (PDOS) of the surface layer with the defect pair $Cd_{Cu}^{+} + V_{Cu}^{-}$ and the third layer without the defect pair. The third layer has no defect, and it is considered as the bulk CIS to facilitate comparisons. The PDOS curve of the surface layer is aligned with that of bulk CIS, and the top of valence band of bulk CIS is set as an energy reference. In Figure 5(a), it can be seen that in the surface layer the valence band maximum (VBM) has a left shift (the calculation shows that the shift is about 0.1 eV). This is because of the lack of copper which weakens the repulsions between Cu-d and Se-p orbitals and depress the valence band. The introduction of the Cd atoms brings a strong repulsion between Cd-d and Se-p orbitals and results in a sharp peak at −9.29 eV. The position of the peak is located at lower energy levels and has little influence on the VBM.

Figure 5(b) shows the PDOS of Cd, In, and Se atoms in the surface layer. The DOS of the third layer is also shown in the figure (marked by "CIS") for comparison. It can be seen that the density of states from the In atoms are higher than those of the Cd atoms in upper energy levels. It means that the In atoms have more important influences on the electronic structure of CIS than the Cd atoms. However, for perfect CIS or Cu-poor CIS, the Cu-Se bonds play the most important role in forming the electronic structure [7].

4. Discussion

For single defect Cd_{Cu}, the Cd atoms might migrate into the deeper positions in the CIS thin film. However, because there are many Cu vacancies at the surface layer, Cd_{Cu} is easier to form the defect pair $Cd_{Cu}^{+} + V_{Cu}^{-}$ with Cu vacancies at the surface (112). They have the lowest formation energy due to the electrostatics interactions between the defect Cd_{Cu} and V_{Cu}. The interaction reduces the formation energy through two ways: (1) the transfer of one electron from the high-energy donor level to low-energy acceptor level and (2) a strong electrostatic attraction between the two charged defects [15]. So most of the Cd atoms from the CdS buffer layer prefer to stay at the (112) surface of CIS to form defect pairs. The diffusion of Cd atoms is localized in a narrow region, and the concentration of Cd at the surface layer is higher than that at deeper layers [31–33].

For the (112) surface of CIS, the formation energy of defect pair $Cd_{Cu}^{+} + V_{Cu}^{-}$ is lower than that of the single defect Cd_{Cu}. The existence of many Cu vacancies makes Cd_{Cu} appear in the form of defect pair $Cd_{Cu}^{+} + V_{Cu}^{-}$ and results in that

the electrons from Cd_{Cu} are accepted by V_{Cu}. So there is no accumulation of electrons at the surface, and this has little influence on the band structure and the carrier transportation.

The electronic structure of CIS is mainly influenced by Cu-Se and In-Se bonds. Because of the lack of Cu atoms at the surface, the repulsions between Cu-d and Se-p orbitals is weakened, and the valence band is depressed. This results in the down shift of the VBM. The antibonding states of Cd-Se bonds are located at the lower energy levels far from the VBM (shown in Figure 5), so a doped Cd atom by itself does not significantly influence on the electronic structure, but the defect pair $Cd_{Cu}^{+} + V_{Cu}^{-}$ plays an important role.

If we consider $CuInSe_2$ (112)/CdS as interface, the down shift (about 0.1 eV) of the VBM caused by the defect pair $Cd_{Cu}^{+} + V_{Cu}^{-}$ will bring a hole barrier. The hole barrier can prevent the holes from approaching the interface and allow electrons to pass through it. This can reduce the recombination of carriers and is conducive to improve the performance of the thin film solar cells.

To explain the reason of the replacement of Cu by Cd, it is helpful to consider the electronegativities of Cu and Cd. The electronegativity of atom Cd ($\chi = 1.69$) is lower than that of atom Cu ($\chi = 1.90$), and so the chemical potential of its electron is higher than that of Cu atom [34]. Because the Se atom has higher electronegativity (lower chemical potential of electron) than Cu and Cd, the difference in chemical potential makes it easier to drive the electrons of Cd to transfer to Se and form Cd-Se bonds. This may be the reason why the atom Cd can substitute Cu in CIS films.

It should be pointed out that the substitution of Cu by Cd in the CIS films is different from the replacement of Cu by Zn [35]. In the latter case, Zn atoms bring additional electrons and form an n-type region near the surface of the CIS films. This results in a bent energy band and prevents the transportation of holes. For the single defect Cd_{Cu}, it has similar effects on the band structure and the transportation of carriers. However, in CIS films, the defect Cd_{Cu} prefers to form the defect pair $Cd_{Cu}^{+} + V_{Cu}^{-}$ with Cu vacancy due to their low formation energy, and their concentration is much higher than that of the single defect Cd_{Cu}. In this case, the additional electron of Cd atom is accepted by Cu vacancy, so the bent band and n-type region are not formed. Therefore, unlike the replacement of Cu by Zn, the substitution of Cu by Cd has little effect on the band structure and the transportation.

5. Conclusion

In this paper, we investigate the doping behaviors of Cd atoms in $CuInSe_2$ thin films. It is found that the Cd atoms prefer to stay at the surface in the form of defect pair $Cd_{Cu}^{+} + V_{Cu}^{-}$ which has the lowest formation energy and is formed easily. The defect pair brings a down shift of valence band maximum about 0.1 eV, which form a hole barrier at the $CuInSe_2$/CdS interface, which can prevent holes from arriving at the interface and reduce the carrier recombination.

Conflict of Interests

The authors declare that there is no conflict of interests regarding the publication of this paper.

Acknowledgments

The authors thank the financial support by the Natural Science Foundation of Jiangsu (Grant no. BK2011033) and the Shanghai Supercomputer Center for providing helps in calculation.

References

[1] P. Jackson, D. Hariskos, E. Lotter et al., "New world record efficiency for Cu(In,Ga)Se_2 thin-film solar cells beyond 20%," *Progress in Photovoltaics: Research and Applications*, vol. 19, no. 7, pp. 894–897, 2011.

[2] M. J. Romero, K. M. Jones, J. AbuShama, Y. Yan, M. M. Al-Jassim, and R. Noufi, "Surface-layer band gap widening in Cu(In,Ga)Se_2 thin films," *Applied Physics Letters*, vol. 83, no. 23, pp. 4731–4733, 2003.

[3] A. Rockett, "Surface analysis of chalcopyrite materials for photovoltaics," *Progress in Photovoltaics: Research and Applications*, vol. 20, no. 5, pp. 575–581, 2012.

[4] D. Liao and A. Rockett, "Cu depletion at the $CuInSe_2$ surface," *Applied Physics Letters*, vol. 82, no. 17, pp. 2829–2831, 2003.

[5] H. Mönig, C.-H. Fischer, A. Grimm et al., "Surface Cu-depletion of Cu(In,Ga)Se_2 thin films: further experimental evidence for a defect-induced surface reconstruction," *Journal of Applied Physics*, vol. 107, no. 11, Article ID 113540, 2010.

[6] U. Rau, K. Taretto, and S. Siebentritt, "Grain boundaries in Cu(In, Ga)$(Se, S)_2$ thin-film solar cells," *Applied Physics A: Materials Science and Processing*, vol. 96, no. 1, pp. 221–234, 2009.

[7] S. B. Zhang and S.-H. Wei, "Reconstruction and energetics of the polar (112) and $(\bar{1}\,\bar{1}\,\bar{2})$ versus the nonpolar (220) surfaces of $CuInSe_2$," *Physical Review B—Condensed Matter and Materials Physics*, vol. 65, no. 8, Article ID 081402, 2002.

[8] J. E. Jaffe and A. Zunger, "Defect-induced nonpolar-to-polar transition at the surface of chalcopyrite semiconductors," *Physical Review B: Condensed Matter and Materials Physics*, vol. 64, no. 24, Article ID 241304, 2001.

[9] S. Siebentritt, N. Papathanasiou, J. Albert, and M. C. Lux-Steiner, "Stability of surfaces in the chalcopyrite system," *Applied Physics Letters*, vol. 88, no. 15, Article ID 151919, 2006.

[10] M. V. Kuznetsov, E. V. Shalaeva, A. G. Panasko, and M. V. Yakushev, "XPS and XPD investigation of (1 1 2) $CuInSe_2$ and Cu(InGa)Se_2 surfaces," *Thin Solid Films*, vol. 451-452, pp. 137–140, 2004.

[11] A. Hofmann and C. Pettenkofer, "Stoichiometry and surface reconstruction of epitaxial $CuInSe_2$(112) films," *Surface Science*, vol. 606, no. 15-16, pp. 1180–1186, 2012.

[12] Y. Hinuma, F. Oba, Y. Kumagai, and I. Tanaka, "Ionization potentials of (112) and $(11\bar{2})$ facet surfaces of $CuInSe_2$ and $CuGaSe_2$," *Physical Review B—Condensed Matter and Materials Physics*, vol. 86, no. 24, Article ID 245433, 2012.

[13] P. Xu, S. Chen, B. Huang, H. J. Xiang, X.-G. Gong, and S.-H. Wei, "Stability and electronic structure of Cu_2ZnSnS_4 surfaces: first-principles study," *Physical Review B—Condensed Matter and Materials Physics*, vol. 88, no. 4, Article ID 045427, 2013.

[14] S.-H. Han, F. S. Hasoon, A. M. Hermann, and D. H. Levi, "Spectroscopic evidence for a surface layer in CuIn Se_2: Cu deficiency," *Applied Physics Letters*, vol. 91, no. 2, Article ID 021904, 2007.

[15] S. B. Zhang, S.-H. Wei, A. Zunger, and H. Katayama-Yoshida, "Defect physics of the $CuInSe_2$ chalcopyrite semiconductor," *Physical Review B—Condensed Matter and Materials Physics*, vol. 57, no. 16, pp. 9642–9656, 1998.

[16] J. L. Shay, J. H. Wernick, and B. R. Pamplin, *Ternary Chalcopyrite Semiconductors*, Pergamon, Oxford, UK, 1975.

[17] K. S. Knight, "The crystal structures of $CuInSe_2$ and $CuInTe_2$," *Materials Research Bulletin*, vol. 27, no. 2, pp. 161–167, 1992.

[18] P. Hohenberg and W. Kohn, "Inhomogeneous electron gas," *Physical Review*, vol. 136, no. 3, pp. B864–B871, 1964.

[19] W. Kohn and L. J. Sham, "Self-consistent equations including exchange and correlation effects," *Physical Review*, vol. 140, no. 4A, pp. A1133–A1138, 1965.

[20] D. M. Ceperley and B. J. Alder, "Ground state of the electron gas by a stochastic method," *Physical Review Letters*, vol. 45, no. 7, pp. 566–569, 1980.

[21] J. P. Perdew and A. Zunger, "Self-interaction correction to density-functional approximations for many-electron systems," *Physical Review B*, vol. 23, no. 10, pp. 5048–5079, 1981.

[22] W. Kohn and L. J. Sham, "Self-consistent equations including exchange and correlation effects," *Physical Review*, vol. 140, no. 4A, pp. A1133–A1138, 1965.

[23] D. Vanderbilt, "Soft self-consistent pseudopotentials in a generalized eigenvalue formalism," *Physical Review B*, vol. 41, no. 11, pp. 7892–7895, 1990.

[24] J. Ihm, A. Zunger, and M. L. Cohen, "Momentum-space formalism for the total energy of solids," *Journal of Physics C: Solid State Physics*, vol. 12, no. 21, pp. 4409–4422, 1979.

[25] K. Yoodee, J. C. Woolley, and V. Sa-Yakanit, "Effects of *p-d* hybridization on the valence band of I-III-VI_2 chalcopyrite semiconductors," *Physical Review B*, vol. 30, no. 10, pp. 5904–5915, 1984.

[26] S. Chen, W.-J. Yin, J.-H. Yang, X. G. Gong, A. Walsh, and S.-H. Wei, "Quaternary semiconductors with positive crystal field splitting: potential high-efficiency spin-polarized electron sources," *Applied Physics Letters*, vol. 95, no. 5, Article ID 052102, 2009.

[27] T. Maeda, T. Takeichi, and T. Wada, "Systematic studies on electronic structures of $CuInSe_2$ and the other chalcopyrite related compounds by first principles calculations," *Physica Status Solidi A: Applications and Materials Science*, vol. 203, no. 11, pp. 2634–2638, 2006.

[28] S.-H. Wei and S. B. Zhang, "Defect properties of $CuInSe_2$ and $CuGaSe_2$," *Journal of Physics and Chemistry of Solids*, vol. 66, no. 11, pp. 1994–1999, 2005.

[29] D. Haneman, "Surface structures and properties of diamond-structure semiconductors," *Physical Review*, vol. 121, no. 4, pp. 1093–1100, 1961.

[30] D. Haneman, "Electron paramagnetic resonance from clean single-crystal cleavage surfaces of silicon," *Physical Review*, vol. 170, no. 3, pp. 705–718, 1968.

[31] T. Nakada and A. Kunioka, "Direct evidence of Cd diffusion into Cu(In,Ga)Se_2 thin films during chemical-bath deposition process of CdS films," *Applied Physics Letters*, vol. 74, no. 17, pp. 2444–2446, 1999.

[32] D. Abou-Ras, J. Dietrich, J. Kavalakkatt et al., "Analysis of Cu(In,Ga)$(S,Se)_2$ thin-film solar cells by means of electron microscopy," *Solar Energy Materials and Solar Cells*, vol. 95, no. 6, pp. 1452–1462, 2011.

[33] D. Abou-Ras, G. Kostorz, A. Romeo, D. Rudmann, and A. N. Tiwari, "Structural and chemical investigations of CBD- and PVD-CdS buffer layers and interfaces in Cu(In,Ga)Se_2-based thin film solar cells," *Thin Solid Films*, vol. 480-481, pp. 118–123, 2005.

[34] R. G. Parr, R. A. Donnelly, M. Levy, and W. E. Palke, "Electronegativity: the density functional viewpoint," *The Journal of Chemical Physics*, vol. 68, no. 8, pp. 3801–3807, 1978.

[35] M. Sugiyama, A. Kinoshita, A. Miyama, H. Nakanishi, and S. F. Chichibu, "Formation of Zn-doped $CuInSe_2$ films by thermal annealing using dimethylzinc," *Journal of Crystal Growth*, vol. 310, no. 4, pp. 794–797, 2008.